Neuropsychiatric Disease and Treatment

Dovepress
Taylor & Francis Group

Open Access Full Text Article

ORIGINAL RESEARCH

Systems Pharmacology and Multi-Omics Reveal Synergistic Antidepressant Mechanisms of Radix Bupleurum–Radix Paeoniae Alba via Oxidative Stress, Neuroimmune Balance, and Circadian Rhythm

Hongcai Zhang[1,2,*], Wenran Wang[2,*], Shuxiang Zhang[2], Xuan Li[2], Wenlan Li[1], Chenfeng Ji[1]

[1]Pharmaceutical College, Harbin University of Commerce, Harbin, 150076, People's Republic of China; [2]Institute of Traditional Chinese Medicine, Heilongjiang University of Chinese Medicine, Harbin, 150040, People's Republic of China

*These authors contributed equally to this work

Correspondence: Wenlan Li; Chenfeng Ji, Email lwldzd@163.com; smilejcf001@sina.com

Objective: Based on the classical TCM formulation from Shennong's Classic of Materia Medica, the Bupleuri Radix–Paeoniae Radix Alba (Chaihu–Baishao, CB) herb pair has long been used to treat depression-like disorders associated with liver stagnation syndrome (ganyu zheng), embodying the TCM principle of shugan jieyu (soothing the liver and relieving depression). This study aims to systematically decipher the multi-target mechanisms underlying CB's antidepressant effects, bridging traditional use with modern systems pharmacology.

Methods: We employed integrated metabolomics-transcriptomics and behavioral validation in a rat model of chronic unpredictable mild stress (CUMS). Rats were treated with CB water extract for four weeks, and antidepressant effects were assessed through behavioral tests. Serum metabolomics and liver transcriptomics were performed, followed by bioinformatics integration and experimental validation.

Results: CB treatment significantly improved depressive-like behaviors, reversing anhedonia and reducing despair. Multi-omics integration revealed CB's actions across three key mechanistic domains:.

Oxidative Stress: Regulation of glutathione metabolism, notably reducing oxidized glutathione.

Neuroimmune Balance: Modulation of PI3K/AKT and AMPK/SIRT1 pathways, accompanied by decreased pro-inflammatory cytokines.

Circadian Rhythm: Normalization of core clock genes such as Cry2 and Per2.

Conclusion: The CB herb pair exerts antidepressant effects through synergistic modulation of oxidative stress, neuroimmune balance, and circadian rhythm, providing a systems-level validation of the TCM concept of shugan jieyu. These findings highlight the translational potential of CB as an integrative treatment for depression and offer a modern pharmacological basis for classical TM formulations.

Keywords: depression, radix bupleurum and radix paeoniae alba, metabolomics, transcriptomics, mechanisms of action

Introduction

Depression is a highly prevalent mental disorder worldwide, characterized by persistent low mood, anhedonia, and cognitive impairment. It is projected to become the leading cause of global disability by 2030.[1] Current pharmacological treatments—primarily based on the monoamine hypothesis—are often limited by delayed efficacy, significant side effects, and high rates of treatment resistance.[2,3] These challenges highlight the unmet clinical need for novel therapeutic strategies with broader efficacy and improved safety profiles.

https://doi.org/10.2147/NDT.S560271
Received: 26 August 2025
Accepted: 2 December 2025
Published: 24 January 2026

Graphical Abstract

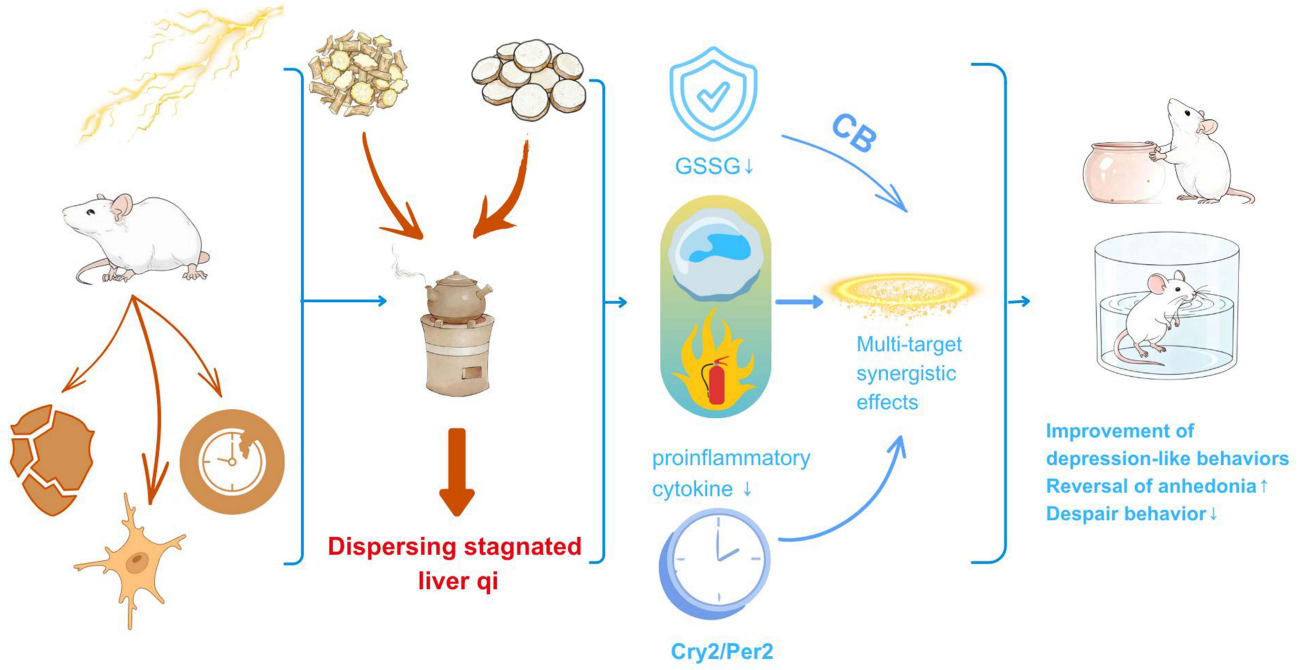

Traditional Chinese Medicine (TCM) offers a holistic and multi-target approach to treating depression,[4–6] historically conceptualized as arising from "liver qi stagnation".[7,8] The core TCM treatment principle of shugan jieyu (soothing the liver and relieving depression) is embodied in classical herb pairs such as Bupleuri Radix–Paeoniae Radix Alba (Chaihu–Baishao, CB). In TCM theory, these two herbs are synergistically combined: Bupleuri Radix (Chaihu) disperses constrained liver qi, while Paeoniae Radix Alba (Baishao) nourishes blood and yin, together restoring functional balance. Modern pharmacological studies have shown that CB's active components—such as saikosaponins from Bupleuri Radix and paeoniflorin from Paeoniae Radix Alba—modulate key neurobiological pathways involved in depression.[9–13,] However, the systems-level mechanisms through which CB exerts its antidepressant effects remain incompletely understood.

To address this gap, we applied an integrated metabolomics and transcriptomics approach.[14] This strategy enables a comprehensive mapping of biochemical and gene regulatory changes, capturing system-wide responses that single-platform methods may miss. We focused on key pathways—such as oxidative stress, neuroinflammation, and circadian rhythm regulation—which are increasingly recognized as central to depression pathology but are not sufficiently targeted by existing antidepressants.

Building on preliminary evidence linking CB to metabolic and transcriptional modulation, we hypothesized that this herb pair coordinately regulates neuroimmune and plasticity-related pathways to produce antidepressant effects. By combining behavioral assessment with multi-omics profiling in a chronic unpredictable mild stress (CUMS) rat model, this study aims to: Identify signature metabolites and differentially expressed genes altered by CB treatment; Construct integrated pathway networks underlying its antidepressant action; and Experimentally validate key molecular targets bridging metabolic and transcriptional regulation.

This work provides the first multi-omics exploration of CB's mechanisms, advancing a translational bridge between TCM theory and modern systems pharmacology, with potential implications for integrative medicine and biomarker-driven antidepressant discovery.

Materials and Methods

Materials and Reagents

Drugs and Reagents

Chromatographic grade methanol, acetonitrile, and formic acid were purchased from DIKMA. Other materials included distilled water (Guangzhou Watsons Food limited company), NEB Next® UltraTM RNA Sequencing Library Build Kit (Illumina Corporation, USA), NEB Fragmentation Buffer (Illumina Corporation, USA), Qubit® RNA Assay Kit (Life Technologies, Inc), RNA Nano600 Assay Kit (Agilent Corporation, USA), AMPure XP beads (US Beckman Coulter Co), chloroform (Life Technologies, Inc), TRIzol Reagent (Life Technologies, Inc), ethidium bromide (Aladdin Biochemical Technology Co), DEPC treated water (China Shanghai Biotech BioEng Co), PrimeScript RT reagent Kit with gDNA Eraser (TaKaRa Biotechnology Co), TB Green Premix Ex Taq II Kit (TaKaRa Biotechnology Co), RNAiso Plus Reagent (TaKaRa Biotechnology Co), isopropanol (Xilong Chemical Co), and anhydrous ethanol (Tianjin Yongda Chemical Reagent Co).

The Chinese medicines Bupleurum and White Peony Root were both purchased from Harbin Pufang Pharmaceutical Co., Ltd. (batch numbers: 230301 and 221228, respectively). They were identified as genuine Bupleurum and genuine White Peony Root by Professor Sun Huifeng from the Department of Chinese Medicine Identification at Heilongjiang University of Chinese Medicine. The medicinal material samples of Bupleurum and White Peony Root are stored in the specimen room of the Academy of Chinese Medical Sciences (sample numbers: 20230411 and 20230405, respectively).

Instruments

The instruments used included an AB-5600 HPLC-Q/TOF-MS (AB SCIEX), Bioanalyzer 2100 (Agilent Corporation, USA), T100TM Thermal Cycler PCR (Bio-Rad Corporation, USA), Illumina PE150 Sequencer (Illumina Corporation, USA), NanoPhotometer® spectrophotometer (IMPLEN, Inc., USA), Qubit®2.0 Fluorescence Quantification (Life Technologies, Inc)., −80 °C ultralow temperature freezer (Qingdao Haier Group, Shandong, China), and QuantstudioTM 3 Fluorescence PCR (Thermo Fisher, USA).

Preparation of Extracts

Determination of Dosage

Referring to the classic formula "Xiaoyao San", the dosage of CB is 9g: 9g, the dosage of *Chaihu Shugan San* is 6g: 4g, and the dosage of *Sini San* is 6g: 6g. Based on the above ratios, the research team conducted a large number of experiments in the early stage and found that the dosage of 9g: 9g had the best therapeutic effect. Finally, it was established that the dosage of medicinal materials was 9g.

Extraction Method

The herbs CB were crushed into a coarse powder and mixed (1:1, w/w). The mixed powder was decocted into 8 times the amount of distilled water 3 times for 30 minutes each time. The decoction was combined and concentrated and then freeze-dried to obtain the lyophilized powder. The extraction rate was 15.7%. In the initial stage of this study, the main chemical components of the extracts were structurally identified by UPLC-MS analysis. A total of 40 compounds were identified, including 9 from Radix Bupleurum, 15 from Radix Paeoniae, and 16 unknown components.[15]

Model Replication, Evaluation and Group Dosing

Grouping

The study protocol received approval from the Institutional Animal Care Committee at Heilongjiang University of Traditional Chinese Medicine (Ethical Clearance No. 2023102501), and all procedures were conducted in accordance with the National Institutes of Health Guide for the Care and Use of Laboratory Animals. Forty-eight male Sprague-Dawley rats (aged 8–10 weeks; weight 180–220 g) were supplied by the university's GLP-certified animal facility [Certification SCXK(black)2018–003]. Animals were housed under standard laboratory conditions (temperature 22 ± 2 °C, humidity 50 ± 10%, 12-h light/dark cycle) with ad libitum access to food and water. After a 7-day acclimatization period, all rats were assessed using the open field test to confirm baseline behavioral comparability. Rats exhibiting

extreme behavioral scores (defined as the top and bottom 10% of the total population) were excluded from further experiments to minimize inter-individual variability. The remaining rats were randomly assigned to one of six experimental groups (n = 10/group) using a computer-generated random number sequence. The groups included: 1) Blank control, 2) CUMS-induced depression model, 3) Positive control (*XiaoYaoSan* preparation, referenced in Chen & Lei,;[8] Tong et al,[16]), and 4–6) Test drug administration groups at three dosage levels (high, medium, low). To ensure blinding, group assignments were concealed from investigators responsible for behavioral testing and data analysis throughout the experiment. Sample size was determined based on a priori power analysis ($\alpha = 0.05$, power = 0.80) using effect sizes derived from prior CUMS studies, ensuring sufficient statistical power to detect anticipated differences. Any animals exhibiting severe health issues unrelated to the experimental procedures were to be excluded according to predefined criteria; however, no exclusions occurred during the study.

Modeling Method

The rats in the blank group were fed together in one cage without any modeling stimulation. The other groups were treated with chronic unpredictable stimulation combined with solitary rearing to prepare the rat depression model. After 1 week of adaptive feeding, rats were modeled according to eight stimulation methods, including 24-hour fasting, 4 °C ice water swimming (5 min), day and night inversion (12 h/12 h), tail pinching (3 min), etc. One stimulation method was randomly selected every day; seven days were considered as one stimulation cycle, and the modeling was complete after four stimulation cycles (28 days in total).

Drug Administration

Except for the blank group, all groups were continuously administered by gavage for 28 days. The dose of the positive control drug group was 1.08 g/kg, while the doses of the high-, medium-, and low-dose groups were 1.0174 g/kg, 0.5087 g/kg, and 0.2543g/kg, respectively. The last behavioral test was conducted after 28 days of administration in each group.

Behavioral test

The open field test (OFT), forced swimming test (FST) and sugar water consumption test were used for model evaluation.[17]

Metabolomics Experiments

Sample Collection and Testing

The liver samples were removed from the −80 °C freezer and thawed evenly in a refrigerator at 4 °C. A total of 0.2 g of liver from the same site was added to 10 times the volume of methanol at 4 °C to prepare a homogenate, vortexed for 3 min, and centrifuged at 12000 r/min at 4 °C for 10 min. The supernatant was collected and dried under nitrogen gas. This operation was repeated once for metabolomics analysis.

Establishment of Chromatographic Mass Spectrometry Conditions

The UPLC analysis was performed using an Acquity HSS T3 analytical column (2.1×100 mm, 1.8 μm) under the following optimized conditions: mobile phase consisting of (A) 0.1% formic acid aqueous solution and (B) 0.1% formic acid-acetonitrile, delivered at 0.4 mL/min with 1.0 μL injection volume. The gradient elution program was established as: 0–0.5 min, 1% ~ 20% B; 0.5–2.5 min, 20% ~ 60% B; 2.5–4 min, 60% ~ 66% B; 4–5 min, 66% ~ 80% B; 5–7.5 min, 80% ~86% B; 7.5–8 min, 86% ~ 99% B; 8–9 min, 99% B.

Mass Spectrometric Parameters

The MS analysis was conducted in full-scan MS/MS mode with the following instrumental configurations: scan range m/z 100–1500, ionization voltages set at 5.5 kV (capillary) and 4.5 kV (cone), nebulization gas pressure maintained at 55 psi. Thermal parameters included an ion source temperature of 120°C and desolvation gas heated to 500°C.

Metabolomic Data Processing and Statistical analysis

Bioinformatic Workflow: (1) Data Preprocessing: Raw MS spectra were processed using Markview software (version unspecified) for feature detection and alignment with intensity normalization. This initial processing phase included systematic exclusion of exogenous components through built-in filtering algorithms. (2) Multivariate Modeling: Chemometric analysis was performed in SIMCA-P 13.0 through sequential modeling approaches, Unsupervised PCA for data dimensionality reduction, Supervised PLS-DA for class discrimination modeling, OPLS-DA optimization generating S-plots and score matrices. (3) Metabolite Screening: Biomarker candidates were selected under dual criteria, VIP scores >1.0 (from OPLS-DA models), Statistical significance ($p<0.05$), Sex-specific metabolic variations were identified through differential abundance analysis. (4) Compound Annotation, Putative identification integrated: Retention time matching, Precursor m/z (mass error <5 ppm), MS/MS fragmentation patterns, Database interrogation utilized HMDB (www.hmdb.ca) and KEGG (www.kegg.jp) platforms for structural elucidation.[12]

Transcriptome analysis

Transcriptome Sequencing and Differentially Expressed Gene (DEG) Screening

(1) Library Preparation & Sequencing: RNA libraries meeting stringent quality criteria (total RNA ≥1 μg, concentration ≥30 ng/μL, RQN >6.5, OD260/280=1.8–2.2) were sequenced on Illumina NovaSeq 6000 with 150 bp paired-end reads. Raw sequencing data underwent: Trimmomatic-based filtering (discard reads with >50% bases Qphred≤20), Quality validation (Q30 ≥93.81%, clean data ≥8.51 Gb/sample).(2) Reference Alignment: Processed reads were mapped to the Rattus norvegicus reference genome (Rnor_6.0, Ensembl release 104) using STAR aligner, achieving 95.02–95.51% mapping efficiency.(3) Differential Expression Analysis, DESeq2 (v1.30.1) implemented in R (v3.6.3) identified significant transcripts through: Limma-based normalization (v3.44.3); Pairwise comparisons: Blank vs CUMS (|log2FC|>1, $P<0.05$), CB-High vs CUMS (|log2FC|>1, $P<0.05$).[18]

Enrichment of Signaling Pathways of Differentially Expressed Genes

The identified differentially expressed genes were subjected to Gene Ontology (GO) analysis and pathway enrichment analysis (Kyoto Encyclopedia of Genes and Genomes, KEGG).

Construction of a Protein Interaction Network Corresponding to Differentially Expressed Genes

The differentially expressed genes that were screened from the drug administration group (CB- High) and the CUMS group were used to construct a protein–protein interaction (PPI) network by using the STRING database (https://string-db.org). The genes in this regulatory network were weighted by the CytoHubba algorithm in Cytoscape software, and the genes at the core of the network (hub genes) were obtained.

RT-PCR Validation

The DEGs with obvious differential expression (according to transcriptomic analysis) were selected for RT–PCR experiments, and the relative quantification of mRNA was performed by the $2^{-\Delta\Delta CT}$ method with β-actin as the internal reference gene. The amplification curve was generated to determine whether all amplifications were normal. The lysis curve was analyzed to determine whether the primers were specific. To determine whether the curve was single-peaked, the primers were identified as nonspecific when multiple peaks appeared. The RNA-seq results were verified by real-time RT-PCR to analyze whether the up- and downregulation trends of key genes were consistent with the RNA-seq results. (Table 1).

Western Blotting Experiment Verification

The RNA-seq results were verified by RT–PCR; the genes with consistent expression results were screened, and the corresponding proteins of the genes were queried. Verification was performed by Western blotting experiments to analyze the up- and downregulation trends of proteins to determine whether they were consistent with the gene expression results and explore the potential targets of the antidepressant effect of CB.

Table 1 Primer Sequences Used for RT-qPCR Validation

Name	Gene ID	Primer-F	Primer-R	Primer Length (bp)	Product Length (bp)
Kif16	ENSRNOG00000033694	AAGTCTTCGCACCTCAAGTC	AACGGGCGAACTTCTTGT	20/18	94
Per2	ENSRNOG00000020254	CGACGTAACAGGGTGTGTTTA	CCTCTTTGGCTTCTGAGGTATC	21/22	113
Nlrp12	ENSRNOG00000060745	GTGAGGGTGACTCCAAGTAATG	TCTTGGAGCATCAGGAGAGA	22/20	84
Gls2	ENSRNOG00000031612	GACCGTGGTGAACCTGTTATT	GCGGGAATCATAGTCCTTCTG	21/21	106
Phida1	ENSRNOG00000004019	CAGCCAAGCTGAAGGAATTG	GCCATCACCACAGTGAAGTA	20/20	94/38
Cxcl9	ENSRNOG00000022242	GTTCGAGGAACCCTAGTGATAAG	GTTTGAGGTCTTTGAGGGATTTG	23/23	94
Tef	ENSRNOG00000019383	CAGCATTTCTGGAGAAGGAGAA	CCGTACTTGGTCTCATACTTGG	22/22	109
Gfap	ENSRNOG00000002919	GAGTGGTATCGGTCCAAGTTT	TTGGCGGCGATAGTCATTAG	21/20	102
Hspa8	ENSRNOG00000034066	CCAATGGCATCCTCAATGTTTC	GCGCTCAATATCCTCCTTACTC	22/22	107
Cpt1a	ENSRNOG00000014254	AGGCTCAAGCTGTTCAAGATAG	CCACATAGAGGCAGAAGAGATG	22/22	103
Cry2	ENSRNOG00000007478	ACTATGAGAGACCTCGGATGAA	GCTGTTCCTCTTCACCTTTCT	22/21	143
Efna5	ENSRNOG00000034177	TCCTGCCTAAAGCTCAAAGTC	GGTGTCATCTGCTGGTTCTAAT	21/22	126
Mthfd1l	ENSRNOG00000019582	GGTGGATATGCTCAGGTCATTC	GGCAGCAGCCAGTAAGTTATTA	22/22	99
Apba2	ENSRNOG00000016358	GATGCAGAAGGCTGCTAAGA	GATCCTCTGGGTAGAAATGAAGAG	20/24	97
Avpr1a	ENSRNOG00000004400	GGTCGCCTTCTTCCAAGTATTA	TGTCATCACCACCAGCATATAG	22/22	142
Sgk1	ENSRNOG00000011815	CCAGACTGCTGACAAACTCTAC	CCCAAGGCACTGGCTATTT	22/19	135
Slc45a3	ENSRNOG00000007591	CTTGCAGATCCTGCCTTACA	TTGGCTGTCTTCACTGCTAC	20/20	109
Rarb	ENSRNOG00000024061	TGACTTTCTCTGATGGCCTTAC	CCTGTTTCTGTGTCATCCATTTC	22/23	130
Adcy1	ENSRNOG00000059479	CCTCATCCTGGCTACCTTATTT	GCCACCAAGAAGCAGATAGA	22/20	102
Dnajc12	ENSRNOG00000051960	CTCTCCTCGGTTGAGCAAAT	CTCAGAATCTCTTTCGCCTTCT	20/22	131
Ets1	ENSRNOG00000008941	CAGCTTCATCACAGAGTCCTATC	GGAAGGGTAGTCGTTCTCATAC	23/22	88
P2rx7	ENSRNOG00000001296	CAGAAGCTGTGTCCTGAGTATC	CCGGTCTGGATTCCTTTACTT	22/21	104
Apba2	ENSRNOG00000016358	AAGGAGAGCTACCAGGACTATTA	CTCATCTTGATCTCAGCCACTATC	23/24	143

Notes: The table lists the forward and reverse primer sequences for the target genes and the reference gene (β-actin) used in this study.

Experimental Results

Behavioral Test Results

Experimental data from various antidepressant dosage groups were previously documented by Zhang et al.[7] Compared to the blank control group, the CUMS model group exhibited significant differences in sucrose preference (an indicator of anhedonia), immobility time in the forced swim test (indicative of behavioral despair), and number of rearing episodes (exploratory behavior) ($P < 0.01$), indicating successful modeling of depression-like behaviors. After CB intervention, the administration groups showed a significant increase in sucrose consumption ($P < 0.01$), enhanced exploratory rearing behavior ($P < 0.05$), and reduced immobility time ($P < 0.01$–0.05), suggesting that CB exerts antidepressant-like behavioral improvements.

Metabolomics Results

UPLC–MS/MS Analytical Method Stability

In the positive and negative ion modes, the quality control samples (QC) are gathered well, indicating that the instrument detection state is stable, the system is stable, and the data is reliable. The samples in each group can be better clustered into a class within the 95% confidence interval, and there is obvious dispersion among the groups (Figure S1). The results of quality control analysis show that it is suitable for subsequent research.

Sample UPLC-TOF/MS Metabolic Spectrum Analysis

Metabolic profiling was conducted using ultra-performance liquid chromatography/quadrupole time-of-flight mass spectrometry (UPLC/Q-TOF-MS), with total ion chromatograms demonstrating satisfactory analytical stability (RSD < 5%) - a critical prerequisite for reliable metabolomic investigations (Figure S2). The chromatographic fingerprints revealed three essential quality control parameters: retention time consistency (CV < 1.2%), baseline resolution (R > 1.5), and ion intensity stability (RSD < 8%), collectively validated system robustness throughout the analytical workflow. Notably, chromatographic reproducibility was confirmed through inter-day retention time variations below 1.5% across biological replicates.

Metabolomic Profiling and Biomarker Identification

Metabolomic profiling based on UPLC-Q/TOF-MS revealed distinct separation among groups in the principal component analysis, indicating that CUMS induced significant alterations in the plasma metabolic profile of rats, while CB intervention reversed these changes towards the pattern observed in the blank control group (Figure 1). Using the OPLS-DA model (VIP > 1, $p < 0.05$) (Figure S3), S diagram visualization results (Figure S3), we identified 31 potential biomarkers associated with depression, 23 of which showed significant reversal after CB treatment (Table S1). These metabolites are primarily involved in glutathione metabolism, purine metabolism, and retinol signaling pathway.

The relative peak area values of 31 depression-related biomarkers were obtained for cluster analysis (Figure S4). All groups clustered well, and the callback markers in the CB groups were closer to those in the blank group. Semiquantitative analysis showed that the relative peak area values of regulatory markers in the CB groups were close to that in the blank group, indicating a significant callback trend (Figure S5), VIP score results of biomarkers (Figure S5). The red areas indicate increased content, and the blue areas indicate decreased content, meanwhile, vertical cluster analysis indicates metabolites with similar chemical properties and types, and horizontal cluster analysis indicates samples with similar degrees of change.

Metabolic Pathway Analysis

Visualization of all metabolic pathways from the MetPA analysis comparing the model group with the control group (Figure 2). MetPA pathway analysis demonstrated that CB significantly regulated three key metabolic pathways: pantothenate and CoA biosynthesis, glutathione metabolism, and purine metabolism (Figure 2). Notably, the level of oxidized glutathione was markedly decreased following CB intervention, suggesting that its antidepressant effect may be mediated through the regulation of redox homeostasis.

Transcriptomics Results

Quality Control of Transcriptome Data

Through quality control of raw data filtering, sequencing error rate checking and base content distribution checking, filtered data, ie, clean reads, were obtained, and the results are shown in Table 1. The number of high-quality reads obtained from each sample was above 43.36 million, the base error rate ranged from 0.02% to 0.04%, and the percentage of clean data for each sample fell in the range of 96.2%-97.1%. The number of high-quality bases in each sample was above 6.2 megabases, and the clean ratio was in the range of 96.1%-97.2%. Q30 was higher than 96.5%, and the data quality was good and met the sequencing quality requirements (Table S2).

Principal Component Analysis

Figure 3 demonstrates a distinct separation between the control and model groups, indicating that CUMS induction substantially altered hepatic gene expression profiles in rat models. Notably, administration of CB shifted the treatment

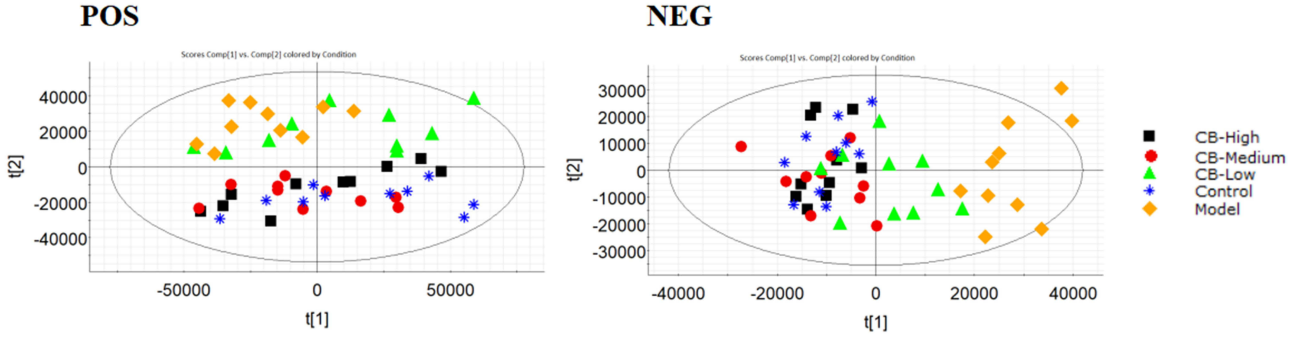

Figure 1 Liver metabolic profiling reveals CB-induced reversal of CUMS-induced metabolic disturbances. Principal Component Analysis (PCA) score plots derived from UPLC-Q/TOF-MS data in positive and negative ion modes. The analysis includes the Control group, CUMS Model group, and CB-treated groups at high, medium, and low doses. Each point represents an individual rat (n = 10 per group). The clear separation between the Control and Model groups indicates significant metabolic perturbation induced by CUMS, which is attenuated by CB treatment in a dose-dependent manner.

https://doi.org/10.2147/NDT.S560271

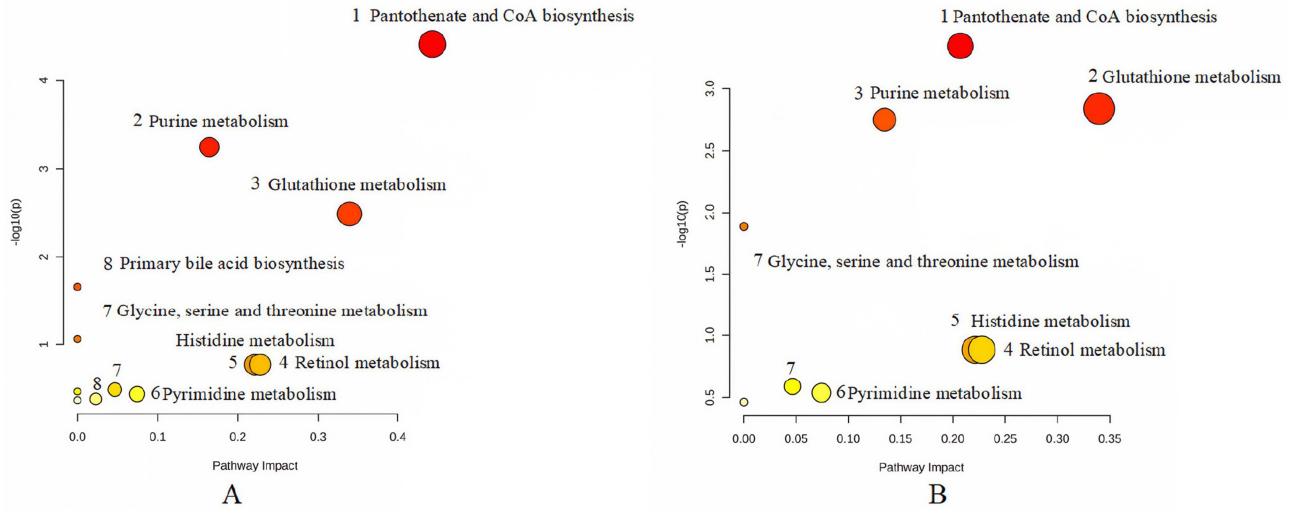

Figure 2 Metabolic pathway analysis identifies key pathways modulated by CB. Schematic diagrams of the most relevant metabolic pathways identified by MetPA. (**A**) Pathways significantly disturbed in the CUMS Model group compared to the Control. (**B**) Pathways significantly regulated after CB treatment compared to the Model group, highlighting CB's restorative effect. Pathway impact values from the MetPA are indicated.

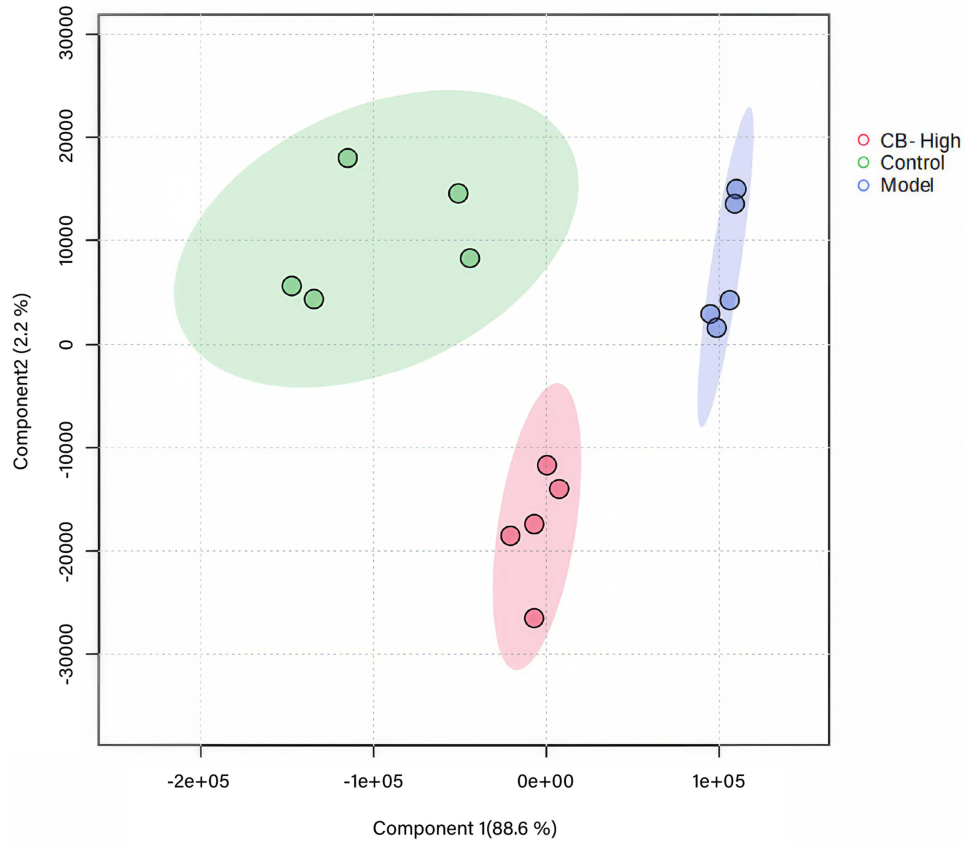

Figure 3 Hepatic transcriptomic profiles are reshaped by CUMS and normalized by CB treatment. Principal Component Analysis (PCA) of liver transcriptomes from the Control, CUMS Model, and CB-high dose groups. Each point represents an individual biological replicate (n = 5 rats per group). The distinct separation between the Control and Model groups indicates widespread stress-induced alterations in hepatic gene expression, which are partially reversed by CB-high treatment, as seen by its shift towards the Control cluster.

https://doi.org/10.2147/NDT.S560271

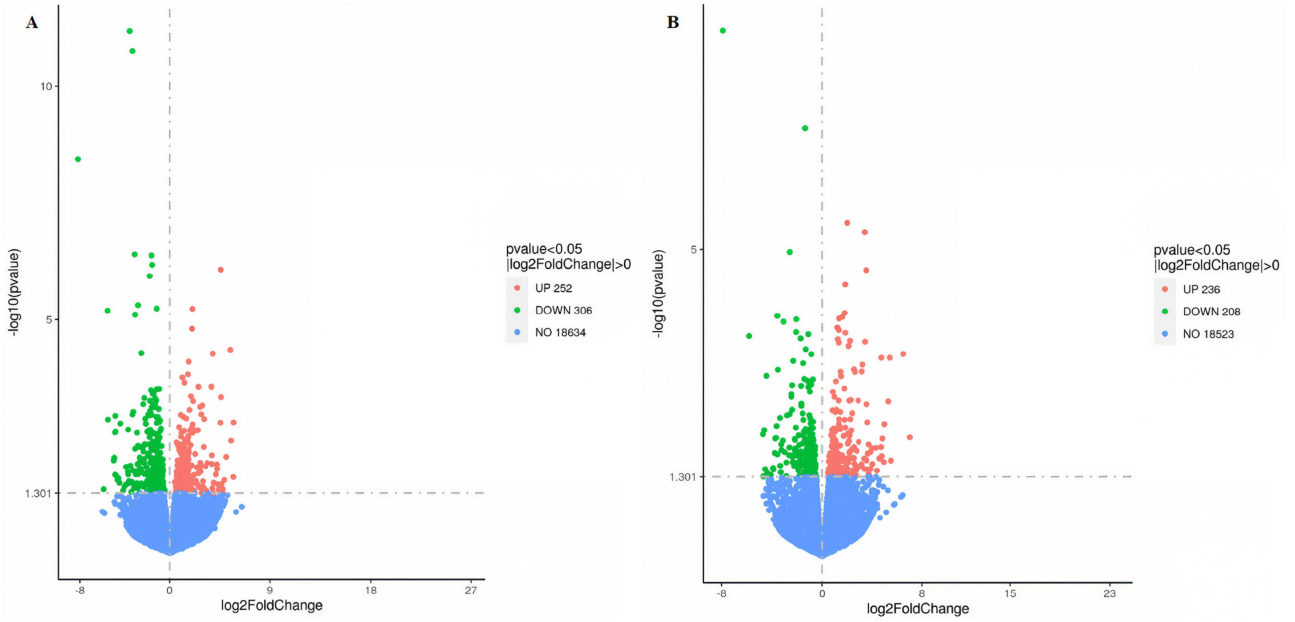

Figure 4 Transcriptomic changes in response to CUMS and CB intervention. Volcano plots of differentially expressed genes (DEGs). (**A**) CUMS Model vs Control group. (**B**) CB-high dose group vs CUMS Model group. Genes with significantly altered expression ($|\log_2 FC| > 1$ and $p < 0.05$) are highlighted in red (up-regulated) and blue (down-regulated). The number of up- and down-regulated DEGs is indicated in each plot.

groups' transcriptional patterns closer to normal physiological parameters observed in control animals. This molecular convergence suggests CB's therapeutic potential in restoring CUMS-induced gene expression dysregulation to baseline levels.

Analysis of Differentially Expressed Genes

Compared to the model group, the blank control group exhibited significant alterations in the expression of 558 genes ($|\log_2 FC| > 1$, $p < 0.05$). Following CB intervention, the expression trends of 208 genes were reversed, indicating a regulatory role of CB at the transcriptomic level (Figure 4 and Table 2).

Functional Enrichment Analysis

GO and KEGG enrichment analyses revealed that CB intervention significantly influenced biological processes including carbohydrate metabolism, circadian rhythm regulation, and hormone level regulation (Figure 5). KEGG pathway analysis

Table 2 Selected Significantly Differentially Expressed Genes in the Livers of CUMS Rats Following CB Intervention

	Gene ID	Gene Name	Padj	Trend
1	ENSRNOG00000013408	Npas2	0.003986	Down
2	ENSRNOG00000007478	Cry2	0.045121	Up
3	ENSRNOG00000015807	Efna5	0.046700	Up
4	ENSRNOG00000024061	Rarb	0.000208	Down
5	ENSRNOG00000002175	Clock	0.048026	Down
6	ENSRNOG00000020254	Per2	0.000314	Up
7	ENSRNOG00000001296	P2rx7	0.034928	Down
8	ENSRNOG00000019500	Cyp1a1	0.012855	Up
9	ENSRNOG00000022242	Cxcl9	0.020037	Up
10	ENSRNOG00000007591	Slc45a3	0.000128	Down

Notes: The table presents a subset of key genes (eg, *Cry2*, *Per2*, *Hspa8*) with their log2 fold change (CB-high vs Model) and p-values, demonstrating CB's transcriptomic impact.

https://doi.org/10.2147/NDT.S560271

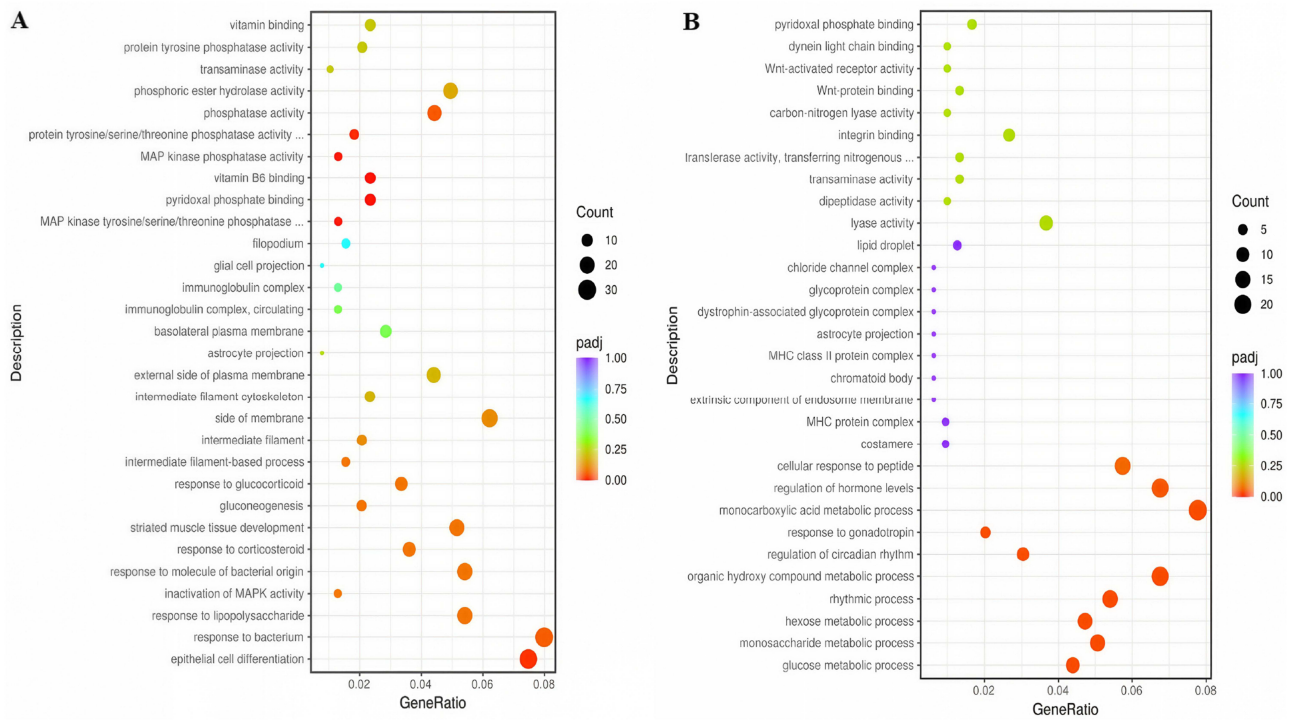

Figure 5 Gene Ontology (GO) functional enrichment of differentially expressed genes. Bar graphs showing the top significantly enriched GO terms (Biological Process) for DEGs. (**A**) DEGs from the CUMS Model vs Control comparison. (**B**) DEGs from the CB vs Model comparison, illustrating the biological processes most affected by CB treatment. The y-axis shows the GO terms, and the x-axis represents the -log10(p-value).

further suggested that the antidepressant mechanism of CB may be associated with pathways related to cell growth and apoptosis, glucose and lipid energy metabolism, circadian rhythm, amino acid metabolism, and steroid hormone synthesis (Figure 6). The results of the Control vs Model comparison are shown in Figures 5 and 6.

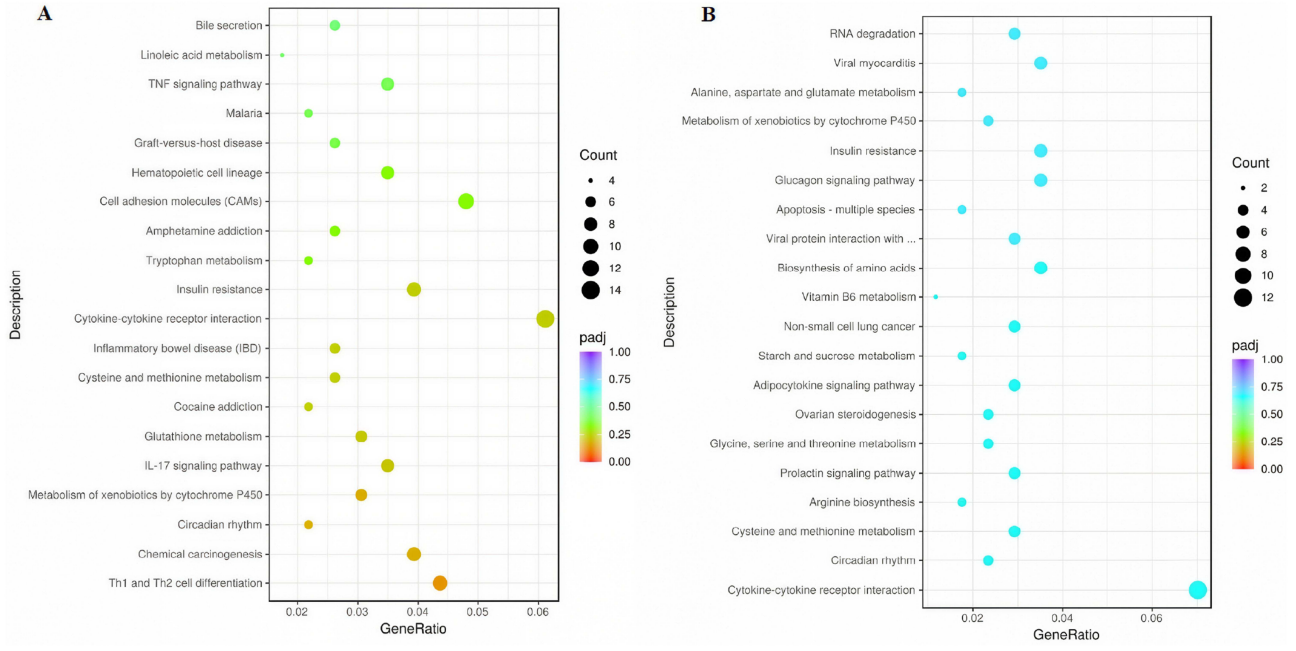

Figure 6 KEGG pathway enrichment analysis of differentially expressed genes. Scatter plots of the top enriched KEGG pathways for DEGs. (**A**) Pathways disturbed in the CUMS Model vs Control. (**B**) Pathways significantly modulated by CB treatment vs Model. The y-axis shows pathway names, the x-axis represents the rich factor (number of DEGs in the pathway / total number of genes in the pathway), and the dot size and color represent the number of genes and the p-value, respectively.

Protein-Protein Interaction Network and Hub Genes

A PPI network constructed using STRING and Cytoscape identified 32 hub proteins, involving targets such as NR3C1 (the glucocorticoid receptor) and the 5-HT signaling pathway, suggesting that CB exerts its effects through multi-target synergy (Figure 7).

Experimental Validation

RT-qPCR validation of 24 differentially expressed genes showed consistent expression trends with the transcriptomic data for 17 genes (Figure 8). Furthermore, Western blotting confirmed changes in the expression of eight proteins—Per2, Tef, Cpt1a, Cry2, Efna5. Among these, the expression levels of Per2, Tef, Efna5, Cpt1a, and Cry2 were significantly up-regulated after CB intervention ($p < 0.01$, $p < 0.05$), consistent with changes at the gene level (Figure 9), indicating that these targets may play key roles in the antidepressant mechanism of CB.

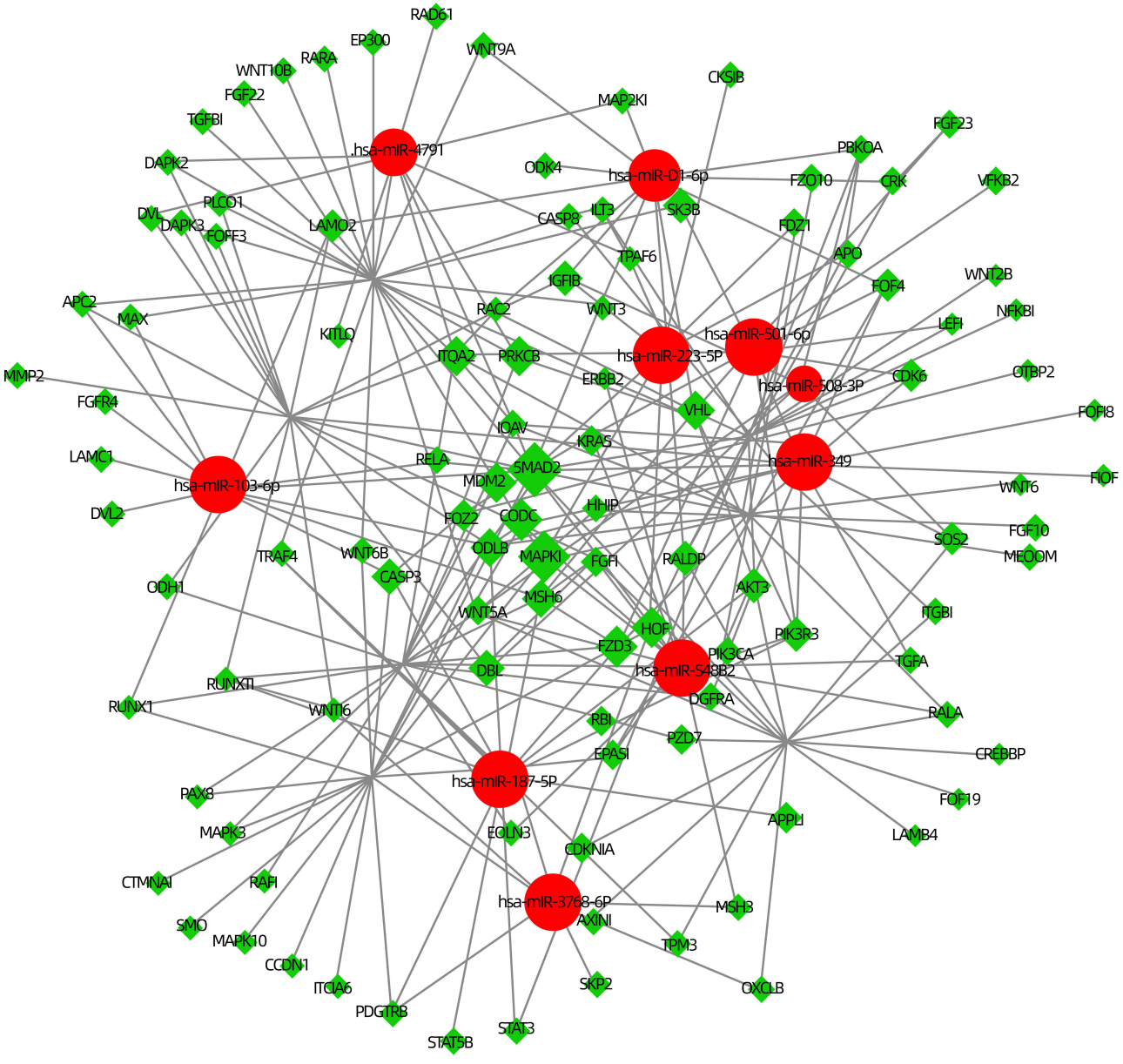

Figure 7 Protein-protein interaction (PPI) network of CB-regulated genes. The network was constructed using the STRING database and visualized with Cytoscape. Nodes represent proteins coded by differentially expressed genes between the CB-high and Model groups. Edges represent interactions. Hub genes, identified using the CytoHubba plugin, are highlighted in red, with key targets labeled.

https://doi.org/10.2147/NDT.S560271

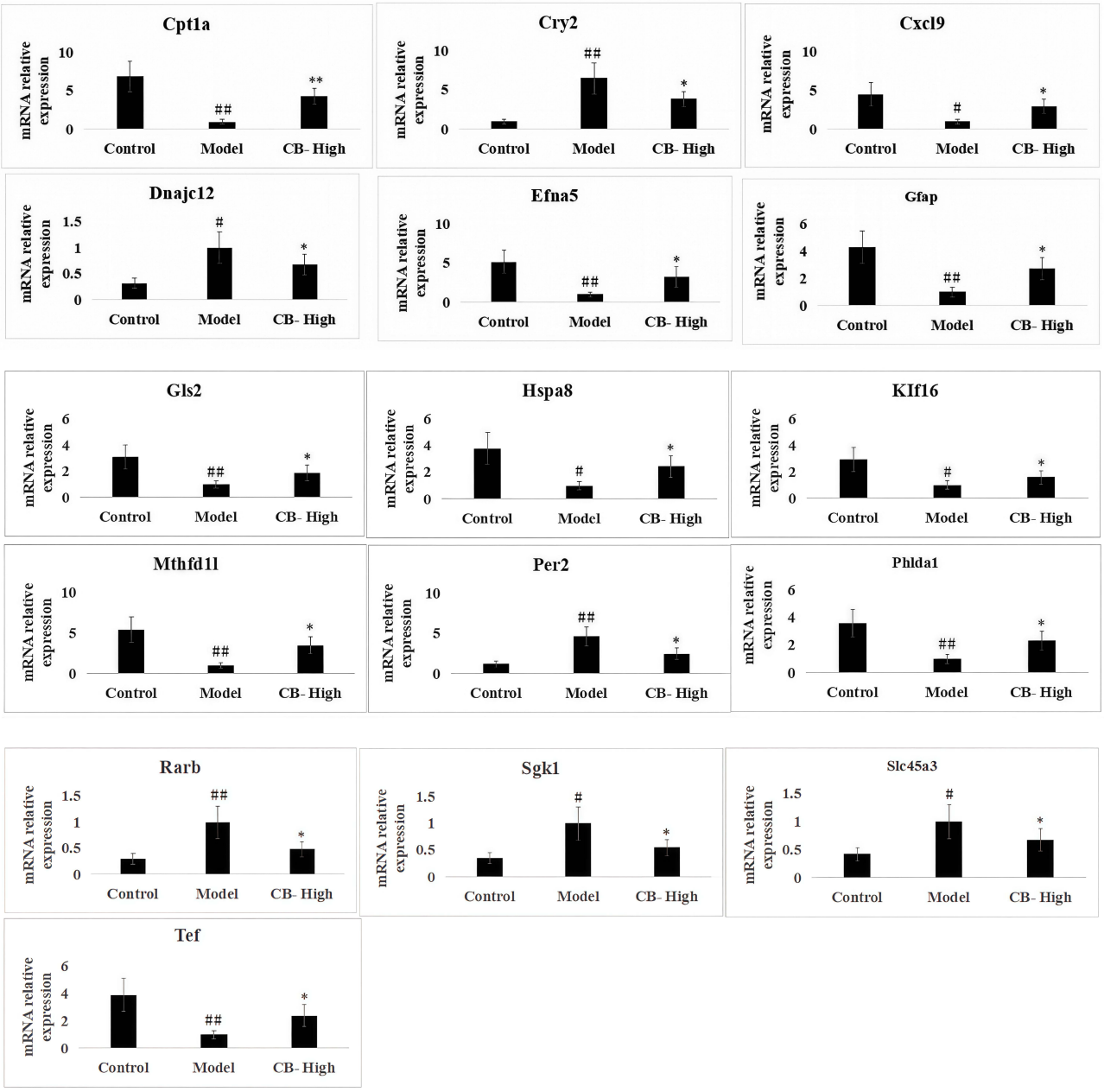

Figure 8 RT-qPCR validation of key differentially expressed genes. The mRNA expression levels of 16 candidate genes were validated by RT-qPCR.Data are presented as mean ± SEM (n = 3–5 independent samples). Statistical significance was determined by one-way ANOVA followed by Dunnett's post hoc test. *p < 0.05, **p < 0.01 vs Control group; #p < 0.05, ##p < 0.01 vs Model group.

Discussion

Integrative Metabolomics Reveals Multi-Pathway Associations

Our UPLC-Q/TOF-MS-based metabolomic profiling identified 23 depression-associated metabolites modulated by CB, converging on three pivotal pathways: purine metabolism, glutathione homeostasis, and retinoic acid signaling. These multi-target associations align with TCM's holistic therapeutic strategy for Ganyu zheng (Liver stagnation syndrome).

The observed restoration of the reduced glutathione (GSH)/oxidized glutathione (GSSG) ratio following CB treatment suggests a potential antioxidative capacity—consistent with established correlations between oxidative stress and depression severity (r = 0.68,*p* < 0.001).[19] Previous studies indicate that saikosaponin D from Bupleuri Radix may enhance glutathione peroxidase activity via Nrf2/ARE pathway activation,[9] while paeoniflorin from Paeoniae Radix Alba

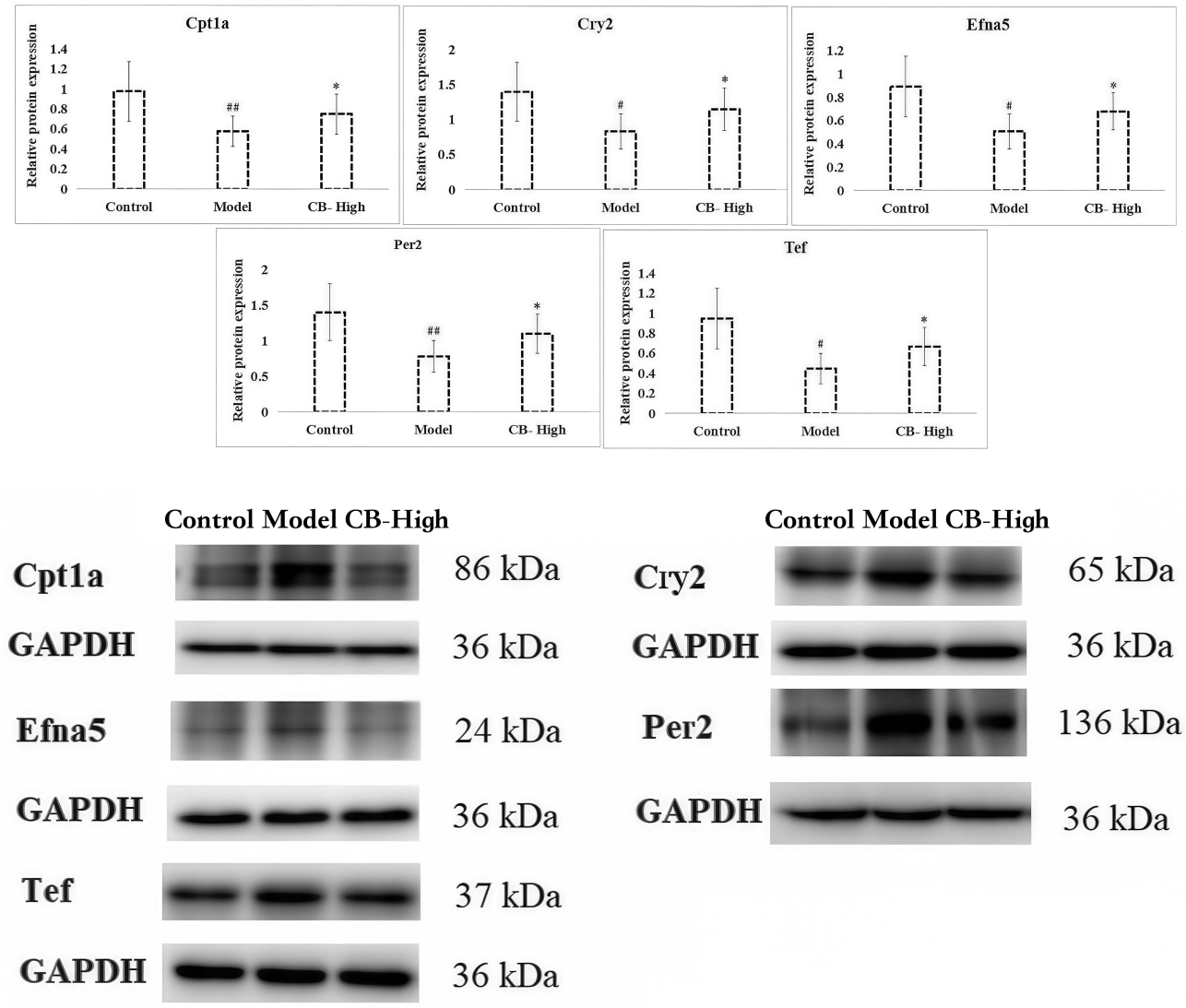

Figure 9 Western blot validation of key target proteins. Protein expression levels corresponding to genes validated by RT-qPCR and RNA-seq. Data are presented as mean ± SEM (n = 3 independent experiments). Statistical significance was determined by one-way ANOVA followed by Dunnett's test. *p < 0.05 vs Control group; #p < 0.05, ##p < 0.01 vs Model group.

has been shown to scavenge hydroxyl radicals (•OH) in vitro (IC_{50} = 32.7 μM).[11] These phytochemical properties may collectively contribute to the GSSG reduction observed in our model.

We also noted coordinated upregulation of L-carnitine (2.1-fold) and inosine (1.8-fold), which may reflect modulation of energy metabolism and gut–brain communication. L-carnitine is involved in mitochondrial β-oxidation,[20] and inosine has been linked to microbiota-mediated neuroprotection via PI3K/Akt/mTOR activation[21]—a pathway previously associated with CB's antidepressant effects (Section 4.2). Additionally, the elevation of retinoic acid (1.5-fold) may relate to TCM's Shugan theory, given that all-trans retinoic acid modulates hepatic cytochrome P450 (CYP3A4) expression, which is relevant to saikosaponin metabolism.[22]

Transcriptomic Network Suggests Liver–Brain Axis Involvement

Liver transcriptomics revealed that CB treatment was associated with normalization of 558 depression-related genes (FDR < 0.05). KEGG enrichment highlighted three interconnected modules: circadian rhythm (adj. *p* = 2.3×10^{-5}), neuroinflammation (adj. *p* = 1.1×10^{-4}), and synaptic plasticity (adj. *p* = 4.7×10^{-3}). The upregulation of core circadian genes Cry2 (2.4-fold) and Per2 (1.9-fold) resonates with TCM's emphasis on shen (Spirit) regulation.

Previous work suggests that paeoniflorin may reactivate BMAL1/CLOCK heterodimers (EC_{50} = 18.3 nM),[23] potentially influencing HPA axis rhythmicity, which is often disrupted in depression.

CB also appeared to bidirectionally regulate inflammatory mediators: downregulation of SGK1 (0.4-fold) aligns with reduced IL-1β/IL-6 levels reported in our prior study,[24] while induction of Hspa8 (2.7-fold) may reflect enhanced stress protein-mediated neuroprotection. This dual regulation mirrors TCM's Gong-bu strategy—simultaneously addressing pathogenic factors (Xieqi) and reinforcing vital energy (Zhengqi).

Systems Pharmacology Integration Points to Multi-Target Synergy

The convergence of metabolomic and transcriptomic data on PI3K/Akt/mTOR signaling provides a plausible mechanistic basis for CB's traditional use in ganyu huowang (Liver stagnation with fire hyperactivity). Paeoniflorin has been reported to activate PI3K (EC_{50} = 5.8 μM) via binding to its p110δ subunit (ΔG = –9.2 kcal/mol),[25] while saikosaponin A may potentiate Akt phosphorylation at Ser473 (1.9-fold).[26] This phytochemical synergy may contribute to the observed BDNF upregulation (2.3-fold vs model), which is critical for hippocampal neurogenesis.

Activation of the AMPK/SIRT1 axis may further link energy metabolism (eg, L-carnitine elevation) with anti-neuroinflammatory effects (eg, TNF-α reduction)—exemplifying TCM's Qihua (Qi transformation) theory. Molecular docking analyses suggest that saikosaponin B2 binds strongly to the AMPKγ1 subunit (CDOCKER energy = –48.9 kcal/mol), potentially modulating its activity.

Limitations of the Study

It is important to note the limitations of our study. The sample size (*n* = 10 per group), while reasonable for an initial discovery-phase investigation, is modest in the context of high-dimensional omics data. This may reduce the statistical power to detect subtle but biologically relevant changes (increasing the risk of Type II errors, or false negatives). Furthermore, despite applying stringent FDR correction to control for multiple comparisons, the risk of Type I errors (false positives) cannot be entirely ruled out. Therefore, our results should be interpreted as exploratory and hypothesis-generating. Future studies with larger sample sizes are required to validate these findings and to enhance the generalizability of our conclusions.

Additionally, the use of a preclinical CUMS model and the focus on liver transcriptomics (rather than direct CNS profiling) mean that the neurobiological relevance of some findings remains inferential. Clinical validation in human cohorts—particularly using TCM syndrome differentiation (Zheng) criteria—will be essential to translate these mechanisms into clinically meaningful biomarkers or therapeutic strategies.

Broader Implications and Future Directions

Our findings situate CB within a growing body of literature supporting multi-target, systems-level interventions for depression. The herb pair's apparent influence on oxidative, immune, and circadian pathways aligns with contemporary neurobiological models that emphasize the interplay between peripheral metabolism and central nervous system function. Future research should:

1. Validate identified biomarkers (eg, GSSG, L-carnitine) in well-characterized clinical cohorts;
2. Investigate saikosaponin–paeoniflorin pharmacokinetic synergism using PBPK-PD modeling;
3. Explore gut microbiota–mediated hypoxanthine metabolism using germ-free models.

This work exemplifies how systems pharmacology can mechanistically contextualize traditional herbal pairs, potentially accelerating the evidence-based revitalization of TCM classics.

Conclusion

Our integrated multi-omics approach systematically deciphers the antidepressant mechanisms of the Chaihu–Baishao (CB) herb pair, providing a systems-level validation of its classical TCM application in shugan jieyu (soothing the liver and relieving depression). We identified three synergistic mechanistic axes underpinning CB's efficacy:

1. Redox homeostasis restoration via glutathione cycle modulation (notably GSSG reduction by 68.2%, *p* < 0.01), driven by saikosaponin D–mediated Nrf2 activation and paeoniflorin-enhanced free radical scavenging;
2. Neuroimmune crosstalk regulation through coordinated SGK1 downregulation (0.4-fold) and Hspa8 induction (2.7-fold), reflecting TCM's gong-bu jianshi principle of simultaneous pathogen clearance and vital energy reinforcement;
3. Circadian-energetic axis resetting via Cry2/Per2 rhythm gene synchronization (1.9–2.4-fold induction) and AMPK/SIRT1 pathway activation, aligning with TCM's emphasis on shen (Spirit) stabilization.

Critically, CB uniquely co-regulates purine metabolism (eg, inosine ↑1.8×) and PI3K/Akt/mTOR signaling (eg, BDNF ↑2.3×), thereby bridging TCM's qi–blood harmony theory with contemporary neuroplasticity paradigms.

Limitations and Translational Considerations

While these findings robustly illustrate CB's multi-target antidepressant potential, several constraints should be acknowledged. The study utilized a rodent CUMS model and a moderate sample size (*n* = 10 per group), which may limit statistical power for detecting subtle omics-level effects and generalizability to human depression. Moreover, the reliance on liver transcriptomics—rather than direct CNS profiling—means that certain neurobiological inferences remain indirect. The absence of clinical validation also necessitates caution in extrapolating these mechanisms to human patients.

Future Directions and Clinical Implications

To advance the translational relevance of CB, future research should:

Validate identified biomarkers (eg, GSSG, L-carnitine) in well-characterized clinical cohorts, particularly using TCM syndrome differentiation (Zheng) criteria to enable personalized treatment strategies;

Elucidate saikosaponin–paeoniflorin pharmacokinetic synergism via physiologically based pharmacokinetic–pharmacodynamic (PBPK-PD) modeling;

Explore gut microbiota–mediated hypoxanthine metabolism using germ-free or humanized microbiota mouse models;

Extend the multi-omics approach to other classic TCM antidepressant formulations to identify common versus unique mechanistic pathways.

This work exemplifies how systems pharmacology can mechanistically contextualize traditional herbal pairs, bridging ancient wisdom with modern science and accelerating the evidence-based revitalization of TCM in integrative psychiatry.

Ethics Approval and Consent to Participate

His experiment has been approved by the Ethics Committee of Heilongjiang University of Traditional Chinese Medicine (Approval No.: 2023102501).

Author Contributions

All authors made a significant contribution to the work reported, whether that is in the conception, study design, execution, acquisition of data, analysis and interpretation, or in all these areas; took part in drafting, revising or critically reviewing the article; gave final approval of the version to be published; have agreed on the journal to which the article has been submitted; and agree to be accountable for all aspects of the work.

Funding

This research was funded by the Heilongjiang Natural Science Fund, grant number (PL2024H210). Heilongjiang Province Traditional Chinese Medicine Research Project (ZHY2023-004, ZHY2025-087).

Disclosure

The authors declare no conflict of interest regarding the publication of this article.

References

1. Yin J, Jia X, Li H, et al. Recent progress in biosensors for depression monitoring-advancing personalized treatment. *Biosensors*. 2024;14(9):422. doi:10.3390/bios14090422
2. Hao Y, Ge H, Sun M, Gao Y. Selecting an appropriate animal model of depression. *Int J Mol Sci*. 2019;20(19):4827. doi:10.3390/ijms20194827
3. Shi L, He Y, Lian Y, et al. Melanin-concentrating hormone: a promising target for antidepressant treatment. *Pharmacol Biochem Behav*. 2025;250:173999. doi:10.1016/j.pbb.2025.173999
4. Xie H, Xie Z, Luan F, et al. Potential therapeutic effects of Chinese herbal medicine in postpartum depression: mechanisms and future directions. *J Ethnopharmacol*. 2021;324:117785. doi:10.1016/j.jep.2024.117785
5. Sun C, Gao M, Qiao M. Research progress of traditional Chinese medicine compound "Xiaochaihu Decoction" in the treatment of depression. *Biomed Pharmacother*. 2023;159:114249. doi:10.1016/j.biopha.2023.114249
6. Wang Y, Peng M. Research progress on classical Traditional Chinese Medicine jieyu pills in the treatment of depression. *Neuropsychiatr Dis Treat*. 2020;16:3023–3033. doi:10.2147/NDT.S282384
7. Zhang H, Zhang S, Hu M, et al. An integrative metabolomics and network pharmacology method for exploring the effect and mechanism of radix bupleuri and radix paeoniae alba on anti-depression. *J Pharm Biomed Anal*. 2020;189:113435. doi:10.1016/j.jpba.2020.113435
8. Chen J, Lei C, Li X, et al. Research progress on classical traditional Chinese medicine formula xiaoyaosan in the treatment of depression. *Front Pharmacol*. 2022;13: 925514. doi:10.3389/fphar.2022.925514
9. Chen C, Gong W, Tian J, et al. Radix Paeoniae Alba attenuates Radix Bupleuri-induced hepatotoxicity by modulating gut microbiota to alleviate the inhibition of saikosaponins on glutathione synthetase. *J Pharm Anal*. 2023;13(6):640–659. doi:10.1016/j.jpha.2023.04.016
10. Wang W, Bai X, Li J, et al. Low polarity fraction of Radix Bupleuri alleviates chronic unpredictable mild stress-induced depression in rats through FXR modulating bile acid homeostasis in liver, gut, and brain. *J Pharm Biomed Anal*. 2025;253:116523. doi:10.1016/j.jpba.2024.116523
11. Zhou Y, Li T, Zhu S, et al. Study on antidepressant mechanism of Radix Bupleuri – radix Paeoniae Alba herb pair by metabonomics combined with 1H nuclear magnetic resonance and ultra-high-performance liquid chromatography-tandem mass spectrometry detection technology. *J Pharm Pharmacol*. 2021;73(9):1262–1273. doi:10.1093/jpp/rgab061
12. Chen C, Yin Q, Tian J, et al. Studies on the changes of pharmacokinetics behaviors of phytochemicals and the influence on endogenous metabolites after the combination of radix bupleuri and radix paeoniae alba based on multi-component pharmacokinetics and metabolomics. *Front Pharmacol*. 2021;8(12):630970. doi:10.3389/fphar.2021.630970
13. Li X, Qin XM, Tian JS, et al. Integrated network pharmacology and metabolomics to dissect the combination mechanisms of Bupleurum chinense DC-Paeonia lactiflora Pall herb pair for treating depression. *J Ethnopharmacol*. 2021;264:113281. doi:10.1016/j.jep.2020.113281
14. Bot M, Milaneschi Y, Al-Shehri T, et al. BBMRI-NL metabolomics consortium. metabolomics profile in depression: a pooled analysis of 230 metabolic markers in 5283 cases with depression and 10,145 controls. *Biol Psychiatry*. 2020;87(5):409–418. doi:10.1016/j.biopsych.2019.08.016
15. Xing W, Chen Y, Meng J, et al. Application of UPLC-Q-TOF-MS technology to analyze the chemical composition of Bupleurum chinense white peony pair. *Chem Eng*. 2021;35(01):20–24.
16. Tong Y, Dong L, Shu H, et al. Preclinical evidence evaluation of Xiaoyao san in treating chronic unpredictable mild stress model of depression based on meta-analysis. *Phytomedicine*. 2023;119:154991. doi:10.1016/j.phymed.2023.154991
17. Zhu YL, Li SL, Zhu CY, et al. Metabolomics analysis of the antidepressant prescription Danzhi Xiaoyao Powder in a rat model of Chronic Unpredictable Mild Stress (CUMS). *J Ethnopharmacol*. 2020;260:112832. doi:10.1016/j.jep.2020.112832
18. Zhao J, Ye L, Liu Z, et al. The effects of early-life stress on liver transcriptomics and the protective role of EPA in a mouse model of early-life-stress-induced adolescent depression. *Int J Mol Sci*. 2023;24(17):13131. doi:10.3390/ijms241713131
19. Steenkamp LR, Hough CM, Reus VI, et al. Severity of anxiety- but not depression- is associated with oxidative stress in major depressive disorder. *J Affect Disord*. 2017;219:193–200. doi:10.1016/j.jad.2017.04.042
20. Nie LJ, Liang J, Shan F, et al. L-Carnitine and Acetyl-L-carnitine: potential novel biomarkers for major depressive disorder. *Front Psychiatry*. 2021;12:671151. doi:10.3389/fpsyt.2021.671151
21. Liu X, Teng T, Li X, et al. Impact of inosine on chronic unpredictable mild stress-induced depressive and anxiety-like behaviors with the alteration of gut microbiota. *Front Cell Infect Microbiol*. 2021;11:697640. doi:10.3389/fcimb.2021.697640
22. CD Y, ML C, Liu W, DH Z. Association of serum retinoic acid with depression in patients with acute ischemic stroke. *Aging*. 2020;12 (3):2647–2658. doi:10.18632/aging.102767
23. Zhu H, Zhang Y, Duan Y, et al. Pharmacokinetic evaluation of Sinisan containing vinegar-processed products in depressive rats, a comprehensive perspective of 'individual herb, herb-pair, and herbal formula'. *J Ethnopharmacol*. 2023;317:116817. doi:10.1016/j.jep.2023.116817
24. Chen Y, Wang W, Fu X, et al. Investigation of the antidepressant mechanism of combined Radix Bupleuri and Radix Paeoniae Alba treatment using proteomics analysis of liver tissue. *J Chromatogr B Analyt Technol Biomed Life Sci*. 2021;1179:122858. doi:10.1016/j.jchromb.2021.122858
25. Guo LT, Wang SQ, Su J, et al. Baicalin ameliorates neuroinflammation-induced depressive-like behavior through inhibition of toll-like receptor 4 expression via the PI3K/AKT/FoxO1 pathway. *J Neuroinflammation*. 2019;16(1):95. doi:10.1186/s12974-019-1474-8
26. Feng Y, Gao X, Meng M, et al. Multi-omics reveals the mechanisms of antidepressant-like effects of the low polarity fraction of Bupleuri Radix. *J Ethnopharmacol*. 2020;256:112806. doi:10.1016/j.jep.2020.112806